Novel Filtering 180° Hybrid Coupler and Its Application to 2 x 4 Filtering Butler Matrix

Shao, Qiang; Chen, Fu-chang; Chu, Qing-xin; Lancaster, Michael J.

DOI:
10.1109/TMTT.2018.2829894

Document Version
Publisher's PDF, also known as Version of record

Citation for published version (Harvard):
Shao, Q, Chen, F, Chu, Q & Lancaster, MJ 2018, 'Novel Filtering 180° Hybrid Coupler and Its Application to 2 x 4 Filtering Butler Matrix', *IEEE Transactions on Microwave Theory and Techniques*, vol. 66, no. 7, pp. 3288 - 3296. https://doi.org/10.1109/TMTT.2018.2829894

Novel Filtering 180° Hybrid Coupler and Its Application to 2 × 4 Filtering Butler Matrix

Qiang Shao, Fu-Chang Chen, *Member, IEEE*, Qing-Xin Chu, *Senior Member, IEEE,* and Michael J. Lancaster, *Senior Member, IEEE*

***Abstract*— In this paper, a novel filtering 180° hybrid coupler is proposed and used to design a 2 × 4 filtering Butler matrix. The filtering 180° hybrid coupler can provide power division and phase shift together with a second-order bandpass transfer function, and is based only on coupled resonators. The 2 × 4 filtering Butler matrix is easily realized by utilizing several hybrid couplers. The analytical synthesis procedures for the hybrid coupler and Butler matrix are presented in this paper. Finally, broadside and end-fire arrays are realized by using the Butler matrix. To illustrate the concept experimentally, a filtering 180° microstrip hybrid coupler and a 2 × 4 filtering microstrip Butler matrix are designed, fabricated, and measured. Simulation and measured results are found to be in good agreement with each other.**

***Index Terms*— Bandpass filter, Butler matrix, hybrid coupler, microstrip, switched-beam antenna.**

I. Introduction

IN RECENT years, with the rapid growth in the use of mobile phones, higher requirements have been put forward for wireless communication systems. In order to achieve higher spectral efficiency and promote the capacity of wireless communication system, problems such as multipath fading and interference become more important. Therefore, smart antennas have been proposed to overcome these problems. In general, there are two different types of smart antenna, one is the adaptive antenna array and the other is the switched-beam antenna array [1]. The former uses digital signal processing to control its pattern, which can enhance the received signal. However, this is difficult to implement into integrated systems because of the high complexity and cost. Compared with adaptive antenna arrays, switched-beam antenna arrays are easier to integrate into systems, and thus, reduce the complexity and cost [1]. The typical switched-beam antenna array is composed of switches, a beam-forming network (BFN), and an antenna array [2]. The switches are used to choose which port is used as the input port, and the BFN splits the input signal and provides phase distribution. The output signals of the BFN feed the antenna array. One BFN is a Butler matrix and it is this network that is enhanced in this paper. Several Butler matrices have been presented for switched-beam antenna arrays in [3]–[5]. In practical use, in order to suppress the spurious frequencies or the intermodulation products generated by amplifiers, separate bandpass filter has to be cascaded before the switches, as shown in Fig. 1(a). The novelty here is to integrate a filter with Butler matrix in order to reduce the size and volume of the system. To do this, Butler matrix is constructed solely of microstrip resonators coupled together to form the filter.

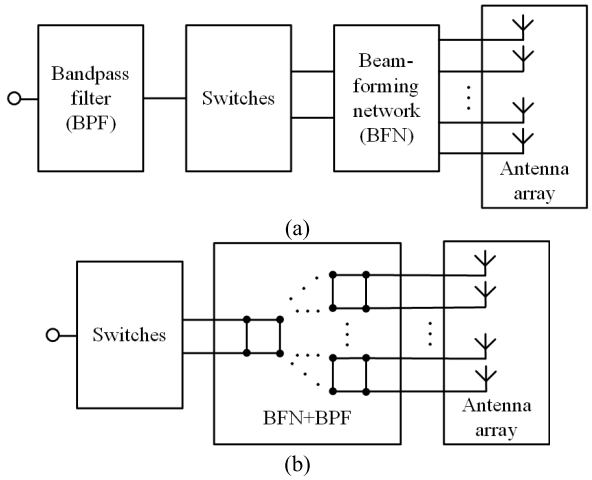

Fig. 1. (a) Basic schematic of a switched-beam antenna with bandpass filter cascaded. (b) Schematic of the Butler matrix based on coupled resonators (large black dots) with filtering transfer functions.

The BFN and bandpass filter are replaced by the new Butler matrix with an inherent bandpass filter function, as shown in Fig. 1(b). Conventionally, the Butler matrix is comprised of hybrid power dividers and phase shifters. Systematic design procedures have been proposed in [6]–[9]. The most common building block to realize Butler matrix is the 90° hybrid coupler, which is a 2×2 hybrid network with equal split of the input power, providing a quadrature phase response across the two outputs [10]. In place of 90° hybrid couplers, a different design procedure using the 180° hybrid couplers have been proposed in [11]. As these hybrid couplers are the main blocks of Butler matrix, introducing filtering functions into them is a way to realize Butler matrix with an inherent bandpass filter.

Manuscript received August 4, 2017; revised November 24, 2017; accepted March 30, 2018. Date of publication May 10, 2018; date of current version July 2, 2018. This work was supported in part by the Guangdong Provincial Key Laboratory of Short-Range Wireless Detection and Communication under Grant 2017B030314003, in part by the National Natural Science Foundation of China under Grant 61571194, in part by the Project of the Pearl River Young Talents of Science and Technology in Guangzhou under Grant 201610010095, and in part by the U.K. Engineering and Physical Science Research Council. *(Corresponding author: Fu-Chang Chen.)*

Q. Shao, F.-C. Chen, and Q.-X. Chu are with the School of Electronic and Information Engineering, South China University of Technology, Guangzhou 510641, China (e-mail: chenfuchang@scut.edu.cn).

M. J. Lancaster is with the School of Electronics, Electrical and Systems Engineering, University of Birmingham, F-87060 Birmingham, U.K.

Color versions of one or more of the figures in this paper are available online at http://ieeexplore.ieee.org.

Digital Object Identifier 10.1109/TMTT.2018.2829894

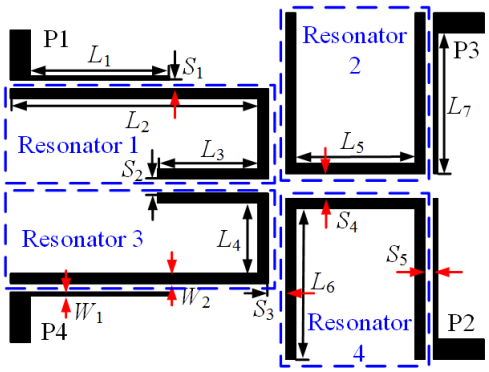

Fig. 2. Layout of the 180° hybrid coupler. ($L_1 = 13.8$ mm, $L_2 = 24.6$ mm, $L_3 = 10$ mm, $L_4 = 7$ mm, $L_5 = 11.8$ mm, $L_6 = 15$ mm, $L_7 = 14$ mm, $W_1 = 0.4$ mm, and $W_2 = 1$ mm.)

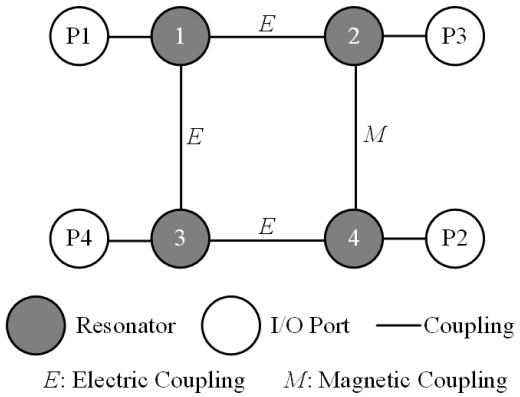

Fig. 3. Coupling scheme of the filtering 180° hybrid coupler.

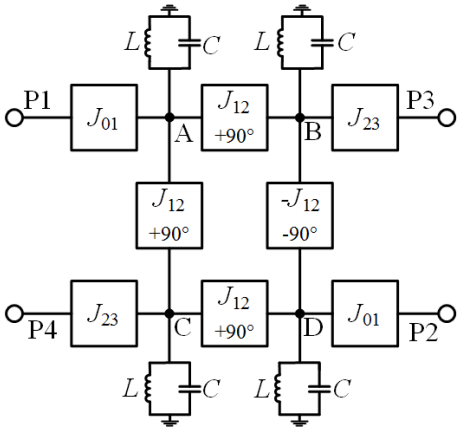

Fig. 4. Equivalent circuit of the 180° hybrid coupler.

Work has been done on introducing filtering functions into the hybrid coupler previously in [12]–[17]. Also, in [18], multiport power dividers with inherent bandpass filter functions were presented by using a hybrid network based on coupled resonators. Other work, which use coupled resonator structures to combine power division with a bandpass filter function, has been presented in [19]–[22]. Crestvolant *et al.* [23] presented a novel class of Butler matrix with inherent bandpass filter transfer functions, which can be applied in multiport power amplifiers.

In this paper, prototypes of a filtering 180° hybrid coupler and a 2 × 4 filtering Butler matrix based on resonators are presented. The analytical synthesis procedures for the hybrid coupler and Butler matrix are given in this paper, and an example filtering 180° microstrip hybrid coupler and a 2 × 4 filtering microstrip Butler matrix are designed, fabricated, and measured. Good agreement has been found between the simulation and measured results, confirming the correctness of the analytical synthesis method.

The remainder of this paper is organized as follows. The detailed design procedure of the 2 × 2 filtering hybrid coupler is given in Section II. In Section III, a 2 × 4 filtering Butler matrix utilizing the hybrid couplers is designed, fabricated, and measured. Good agreement has been obtained between the simulation and measured results. Last, Section IV concludes this paper.

II. Design of Filtering 180° Hybrid Couplers

Fig. 2 shows the microstrip layout of the proposed filtering 180° hybrid coupler based on coupled resonators. All the four resonators are half-wavelength uniform impedance resonators, which resonate at the central frequency of the bandpass filter (f_0). Fig. 3 shows the coupling scheme of the proposed 180° hybrid coupler. The input ports 1 and 2 are coupled to the resonators 1 and 4, respectively. The output ports 3 and 4 are coupled to the resonators 2 and 3, respectively. Furthermore, all the coupling strengths between adjacent resonators are equal numerically. However, the couplings between resonators 1 and 2, 1 and 3, and 3 and 4 are dominated by electric couplings, while the coupling between resonators 2 and 4 is dominated by magnetic coupling [23].

A. Analysis

Different types of coupling between resonators can cause different phase shifts [24], which are shown as follows:

$$\Phi = +90^\circ \text{ (in this case dominated by electric coupling)} \tag{1}$$

$$\Phi = -90^\circ \text{ (in this case dominated by magnetic coupling).} \tag{2}$$

With these considerations, the equivalent circuit of the proposed filtering 180° hybrid coupler can be generated and is shown in Fig. 4. The admittance inverters J_{01} and J_{23} are used to model the input and output coupling. Considering the coupling strength between adjacent resonators and its phase shift, the +90° and −90° admittance inverters J_{12} are used to represent the coupling dominated by electric fields and magnetic fields in Fig. 2. In addition, the four resonators are represented by the same parallel LC resonators.

When the signal is input from port 1, there are two paths to reach port 2; these are path ABD and path ACD. On path ABD, since there is a +90° admittance inverter J_{12} and a −90° admittance inverter J_{12}, the total phase shift of this

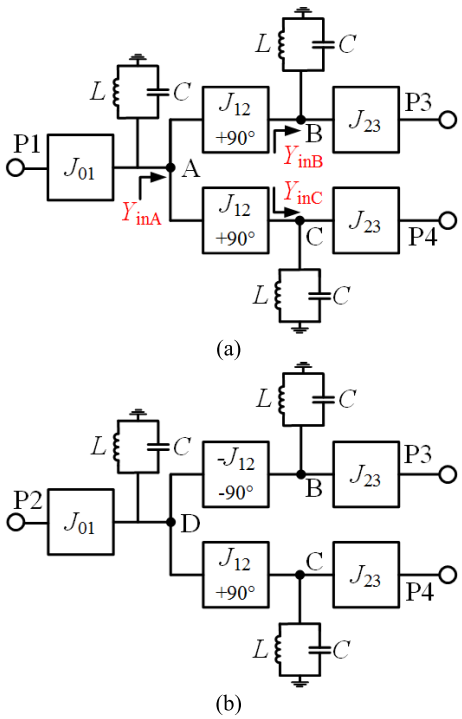

Fig. 5. Equivalent circuit of the 180° hybrid coupler. (a) Input at port 1. (b) Input at port 2.

path is 0°. However, on path ACD there is a total phase shift of 180°. In addition, the coupling strength of these two paths is identical. Thus, the signals travelling on the two paths will cancel out on node D, so in the ideal case there will be no signal output from port 2. Therefore, high isolation between ports 1 and 2 is achieved.

As the signals on the two paths cancel out each other on node D, node D can be equivalent to an open circuit. A new equivalent circuit is shown in Fig. 5(a), where the signal is input to port 1. In the same way, when the signal is input to port 2, a new equivalent circuit can be formed and is shown in Fig. 5(b). From node A in Fig. 5(a), input admittance Y_{inA} is calculated as

$$Y_{\text{inA}} = \frac{J_{12}^2}{Y_{\text{inB}}} + \frac{J_{12}^2}{Y_{\text{inC}}} \tag{3}$$

where Y_{inB} and Y_{inC} are the input admittance from nodes B and C, which are calculated as

$$Y_{\text{inB}} = Y_{\text{inC}} = \frac{J_{23}^2}{Y_0} + j\omega C + \frac{1}{j\omega L}. \tag{4}$$

Therefore, the input admittance Y_{inA} can be calculated as

$$Y_{\text{inA}} = \frac{J_{12}^2}{Y_{\text{inB}}} + \frac{J_{12}^2}{Y_{\text{inC}}} = 2\frac{J_{12}^2}{Y_{\text{inB}}} = \frac{(\sqrt{2}J_{12})^2}{Y_{\text{inB}}}. \tag{5}$$

Based on (5), the equivalent circuit shown in Fig. 5(a) can be further simplified into a two-port network shown in Fig. 6. This is a second-order bandpass filter using admittance inverters. In the same way, the equivalent circuit shown in Fig. 5(b) can also be simplified into the second-order bandpass filter in Fig. 6. In summary, when the signal is input from port 1,

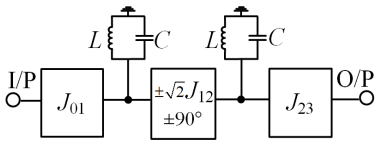

Fig. 6. Equivalent circuit of the coupled resonator bandpass filter.

it is equally split into the output ports 3 and 4 with equal phase shift. When the signal is input from port 2, it is equally split into the output ports 3 and 4 with a 180° phase shift. In addition, each path from the input port to output port is equivalent to a second-order bandpass filter. Therefore, the whole circuit is a filtering 180° hybrid coupler.

Since the equivalent circuit in Fig. 6 is a second-order bandpass filter using admittance inverters, it can be synthesized by using a conventional technique [25]. Once the design requirements, such as center frequency (f_0), fractional bandwidth (FBW), and ripple level are given, the element values for low-pass prototype filter can be obtained. Having obtained the low-pass prototype parameters, the bandpass design parameters can be calculated as follows [25]:

$$Q_{e1} = \frac{g_0 g_1}{\text{FBW}} \quad Q_{e2} = \frac{g_2 g_3}{\text{FBW}} \tag{6}$$

$$M_{12} = \pm\frac{\sqrt{2}\text{FBW}}{2\sqrt{g_1 g_2}} \tag{7}$$

where Q_{e1} and Q_{e2} are the external quality factors of the resonators at the input and output, and M_{12} is the coupling coefficient between the adjacent resonators. ("+" is taken when the coupling is dominated by electric coupling, and "−" is taken when the coupling is dominated by magnetic coupling.)

B. Synthesis

In order to verify the analysis above, a microstrip filtering 180° hybrid coupler is designed, fabricated, and measured. The circuits are fabricated on a substrate with dielectric constant $\varepsilon_r = 2.55$, loss tangent $\delta = 0.0029$, and thickness $h = 0.8$ mm. The center frequency of the filter is taken to be 2.4 GHz with a FBW of 2.5%. The ripple level is designed to be 0.04321 corresponding to a 20-dB return loss. Therefore, the element values for low-pass prototype filter can be obtained as $g_1 = 0.6648$, $g_2 = 0.5445$, and $g_3 = 1.2210$. Based on (6) and (7), the external quality factors can be easily calculated as $Q_{e1} = Q_{e2} = 26.6$, and the coupling coefficient between adjacent resonators is calculated as $M_{12} = \pm 0.029$.

Fig. 7 shows the extracted input and output external quality factors with respect to the gap from the ports to the input and output resonators (S_1 and S_5). These are obtained by following the technique described in [25]. From the graph, the initial values of the gaps between the resonators and feeding lines can be easily obtained as $S_1 = S_5 = 0.33$ mm. Similarly, the extracted coupling coefficients with respect to the gaps S_2, S_3, and S_4 are shown in Fig. 8. The initial values of the gaps between adjacent resonators can now be easily obtained as $S_2 = 0.9$, $S_3 = 1.24$, and $S_4 = 1.94$ mm. In order to improve the overall response, the final dimensions of the

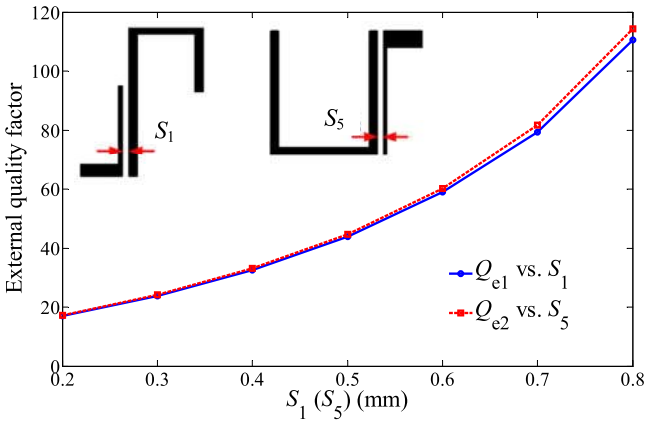

Fig. 7. Extracted external quality factor with respect to the corresponding physical parameters.

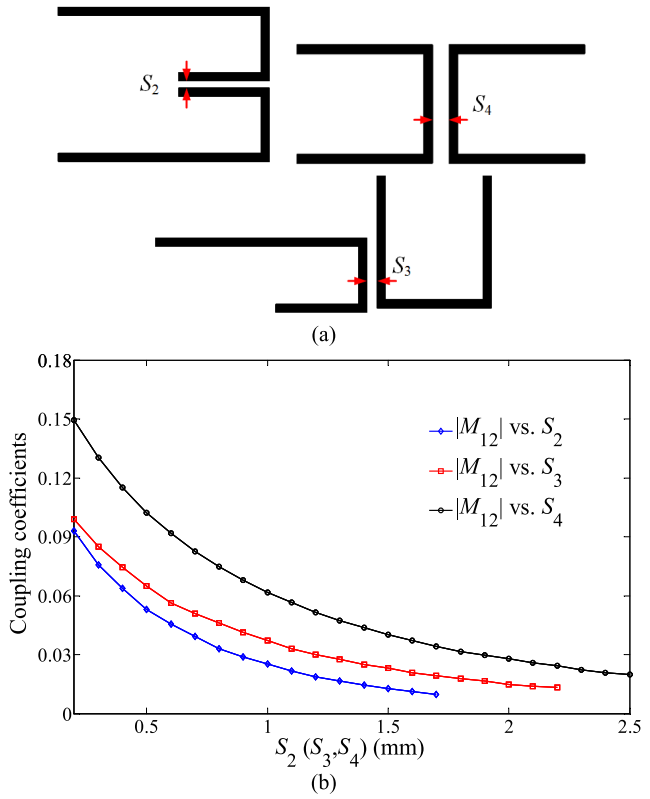

Fig. 8. (a) Circuit layout for extracting coupling coefficients $|M_{12}|$. (b) Extracted coupling coefficients with respect to the corresponding physical parameters.

gaps in Fig. 2 are optimized in IE3D software as $S_1 = 0.35$, $S_2 = 0.9$, $S_3 = 1.25$, $S_4 = 2$, and $S_5 = 0.35$ mm. The small differences between the initial and optimized values show the high accuracy of the technique.

C. Measurement Results

Fig. 9 shows a photograph of the fabricated filtering 180° hybrid coupler. Fig. 10(a) and (b) shows the simulated and measured S-parameters of the filtering 180° hybrid coupler when the signal is input to ports 1 and 2, respectively. It can be clearly observed that the measured results are in

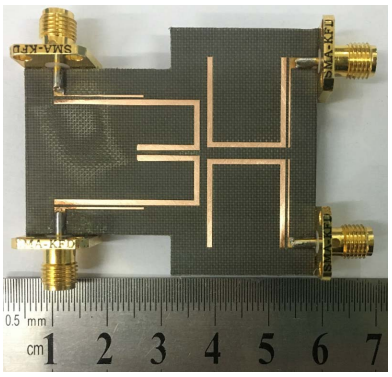

Fig. 9. Photograph of the fabricated filtering 180° hybrid coupler.

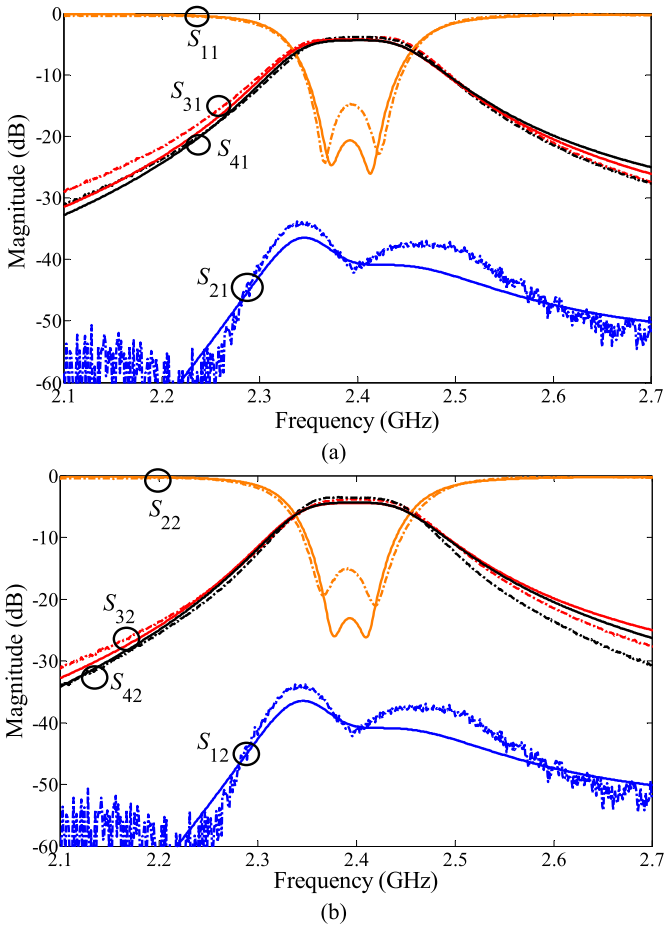

Fig. 10. Simulated and measured S-parameters of the fabricated filtering 180° hybrid coupler. (Solid lines: simulation results and dashed-dotted lines: measured results). (a) S_{11}, S_{31}, S_{41}, and S_{21}. (b) S_{22}, S_{32}, S_{42}, and S_{12}.

good agreement with the simulation results. The measured minimum insertion loss for the bandpass filter is 4.2 dB, which includes the 3-dB power splitting ratio and 1.2-dB filter loss. The return losses are lower than 14.7 dB, which are line with the tolerances of the manufacturing technique. The measured isolation between ports 1 and 2 is larger than 34 dB. The measured output phases of the coupler are shown in Fig. 11, showing, as expected, $\angle S_{31}$, $\angle S_{41}$, and $\angle S_{32}$ in phase and $\angle S_{42}$ out of phase. Within the 3-dBFBW

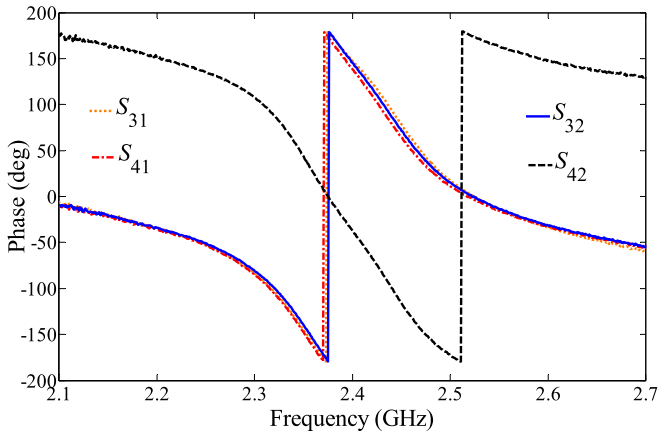

Fig. 11. Measured output phase of the fabricated filtering 180° hybrid coupler.

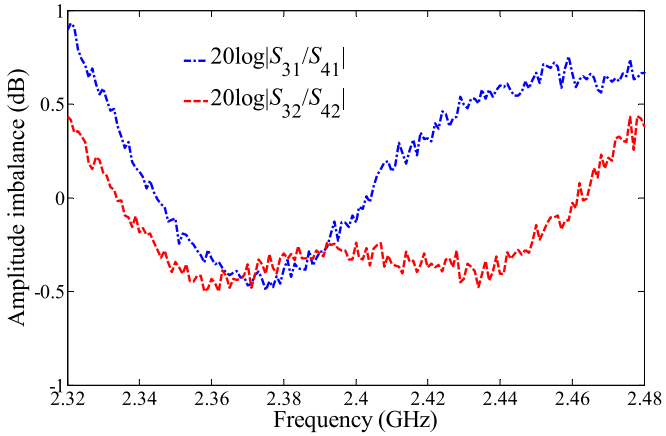

Fig. 12. Measured output amplitude error of the fabricated filtering 180° hybrid coupler.

(2.34–2.46 GHz) of the filter, the measured phase imbalances are within±6°. The measured amplitude imbalances of the coupler are shown in Fig. 12, and here the difference of output amplitude responses $S_{31} - S_{41}(S_{32} - S_{42})$ is shown. The measured amplitude imbalances are lower than ±0.8 dB within the 3-dB bandwidth of the bandpass filter.

III. Design of the 2 × 4 Filtering Butler Matrix

Since the 180° hybrid coupler is the fundamental building block of Butler matrix, it can be utilized to design a filtering Butler matrix. The filtering 180° hybrid coupler [Fig. 13(a)] can be used to design a 2 × 4 Butler matrix [Fig. 13(b)]. The microstrip layout and the coupling diagram can be seen in Fig. 14. When port 1 is used as the input port, it can be easily observed that the output ports (ports 3–6) have equal amplitude and phase shift. When port 2 is used as the input port, the output port phases can be calculated as

$$\begin{aligned}\angle S_{42}-\angle S_{32} &= (\angle S_{C2}+\angle S_{\rm DC}+\angle S_{4D})-(\angle S_{A2}+\angle S_{\rm BA}+\angle S_{3B})\\ &= (\angle S_{C2}-\angle S_{A2})-(\angle S_{\rm DC}-\angle S_{\rm BA}) \quad (8)\\ \angle S_{52}-\angle S_{42} &= (\angle S_{A2}+\angle S_{\rm BA}+\angle S_{5B})-(\angle S_{C2}+\angle S_{\rm DC}+\angle S_{4D})\\ &= (\angle S_{A2}-\angle S_{C2})-(\angle S_{\rm BA}-\angle S_{\rm DC}) \quad (9)\\ \angle S_{62}-\angle S_{52} &= (\angle S_{C2}+\angle S_{\rm DC}+\angle S_{6D})-(\angle S_{A2}+\angle S_{\rm BA}+\angle S_{5B})\\ &= (\angle S_{C2}-\angle S_{A2})-(\angle S_{\rm DC}-\angle S_{\rm BA}) \quad (10)\end{aligned}$$

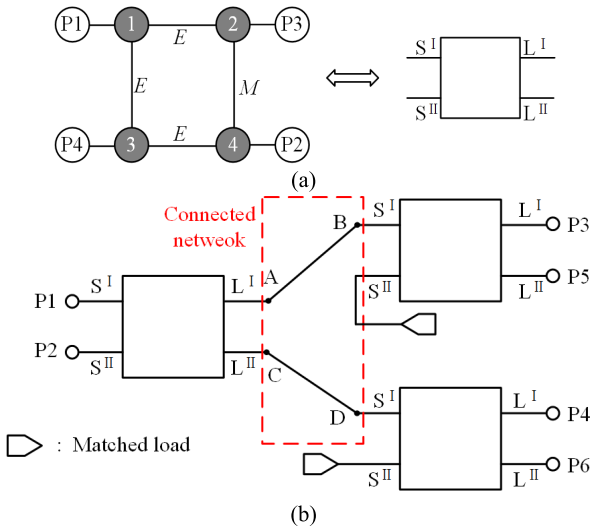

Fig. 13. (a) Schematic of the 2 × 2 fundamental unit. (b) Conventional block diagram of a 2 × 4 Butler matrix by utilizing the 180° hybrid coupler.

where $\angle S_{\rm BA}$ represents the phase response between either a port or one of the nodes A, B, C, D defined in Fig. 13(b), as the connecting network. Based on the properties of the 180° hybrid coupler, the phase response across the output ports of the first coupler is

$$\angle S_{C2} - \angle S_{A2} = 180° \quad (11)$$

$$\angle S_{3B} = \angle S_{5B} \quad \angle S_{4D} = \angle S_{6D} \quad (12)$$

The 2 × 4 filtering matrix is realized by connecting the couplers together via AB and CD and in order to realize the bandpass response. These connections are simply made by coupling together the resonators in the adjoining couplers, as shown in Fig. 14(b). These are made by the electric couplings so that the phase response of the connecting network is

$$\angle S_{\rm DC} = \angle S_{\rm BA} = 90° \quad (13)$$

In general, considering (8)–(13), when port 2 is used as the input port, the output port phases can be calculated as

$$\angle S_{52} = \angle S_{32} \quad \angle S_{42} = \angle S_{62} \quad (14)$$

$$\angle S_{42} - \angle S_{32} = \angle S_{52} - \angle S_{42} = \angle S_{62} - \angle S_{52} = 180°. \quad (15)$$

Based on a similar analysis to that in Section II, each path from an input port to an output port can be equivalent to a fourth-order bandpass filter, as shown in Fig. 15. The bandpass design parameters can thus be calculated as follows [25]:

$$Q_{e1} = \frac{g_0 g_1}{\rm FBW} \quad Q_{e2} = \frac{g_4 g_5}{\rm FBW} \quad (16)$$

$$M_{12} = \pm\frac{\sqrt{2}\,{\rm FBW}}{2\sqrt{g_1 g_2}} \quad M_{23} = \frac{\rm FBW}{\sqrt{g_2 g_3}} \quad M_{34} = \frac{\sqrt{2}\,{\rm FBW}}{2\sqrt{g_3 g_4}} \quad (17)$$

where Q_{e1} and Q_{e2} are the external quality factors of the resonators at the input and output, and M_{12}, M_{23}, and M_{34} are the coupling coefficients between the adjacent resonators. ("+" is taken when the coupling is dominated by electric coupling, and "–" is taken when the coupling is dominated by magnetic coupling.)

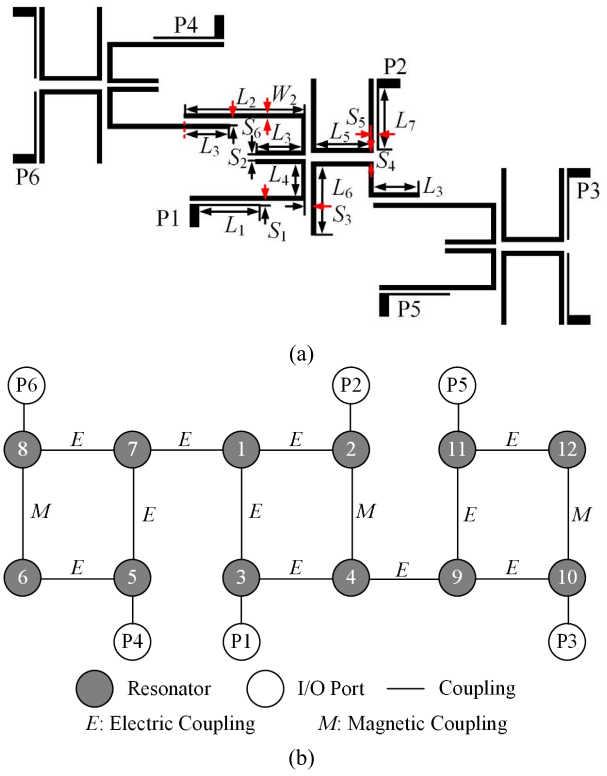

Fig. 14. (a) Layout of the 2 × 4 filtering Butler matrix. ($L_1 = 13.8$ mm, $L_2 = 24.6$ mm, $L_3 = 10$ mm,$L_4 = 7$ mm, $L_5 = 11.8$ mm, $L_6 = 15$ mm, $L_7 = 14$ mm, $W_1 = 0.4$ mm, and $W_2 = 1$ mm). (b) Coupling scheme of the 2 × 4 filtering Butler matrix.

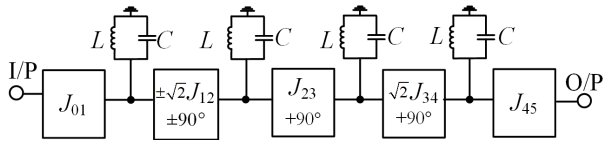

Fig. 15. Equivalent circuit of the coupled resonator bandpass filter.

In order to illustrate the discussion above, a 2 × 4 filtering Butler matrix is designed, fabricated, and measured. The center frequency of the filter is taken to be 2.4 GHz with a FBW of 3.5%. The ripple level is designed to be 0.04321. The element values can be obtained as $g_1 = 0.9314$, $g_2 = 1.2920$, $g_3 = 1.5775$, $g_4 = 0.7628$, and $g_5 = 1.2210$. Based on (16) and (17), the external quality factors can be easily calculated as $Q_{e1} = Q_{e2} = 26.6$, and the coupling coefficients between adjacent resonators are calculated as $M_{12} = \pm 0.023$, $M_{23} = 0.025$, and $M_{34} = 0.023$.

According to Fig. 7, the initial values of the gaps between the feeding lines and resonators can be easily obtained as $S_1 = S_5 = 0.33$ mm in order to meet the required external quality factor. Similarly, the initial values of the gaps between the adjacent resonators can also be obtained as $S_2 = 1.05$, $S_3 = 1.50$, $S_4 = 2.25$, and $S_6 = 1.4$ mm according to Fig. 8. The final dimensions of the gaps in Fig. 14(a) are optimized in IE3D software as $S_1 = 0.35$, $S_2 = 0.9$, $S_3 = 1.25$, $S_4 = 2$, $S_5 = 0.35$, and $S_6 = 1.25$ mm.

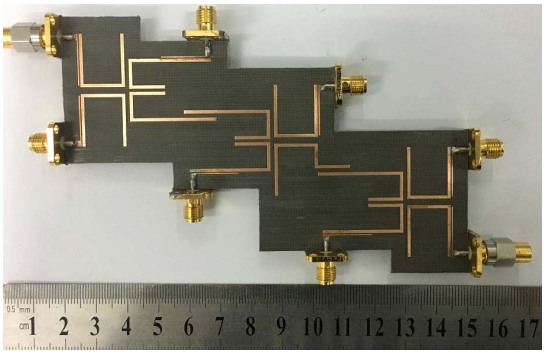

Fig. 16. Photograph of the fabricated 2 × 4 filtering Butler matrix.

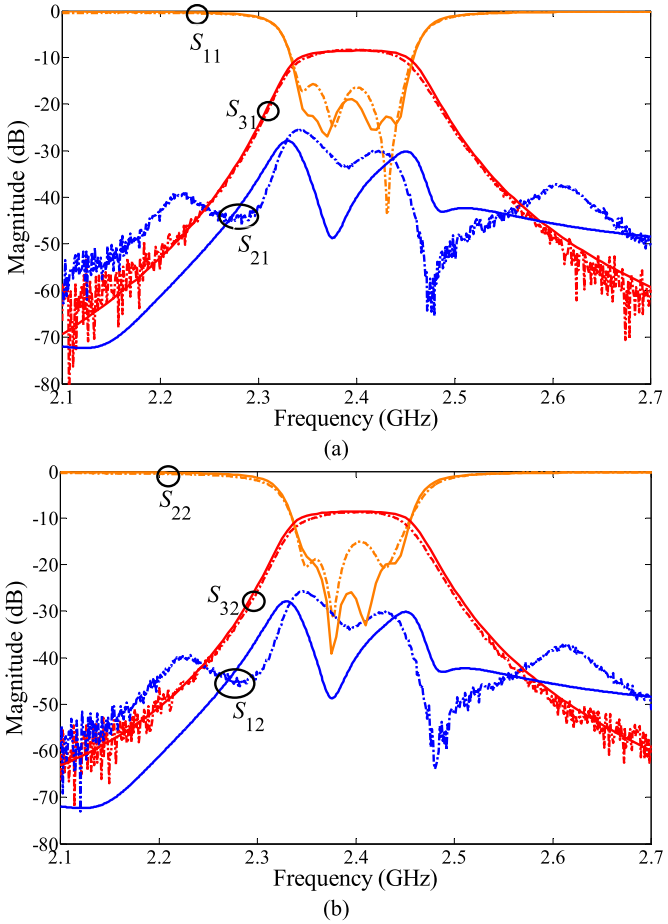

Fig. 17. Simulated and measured S-parameters of the fabricated filtering 2×4 filtering Butler matrix. (Solid lines: simulation results and dashed–dotted lines: measured results). (a) S_{11}, S_{31}, and S_{21}. (b) S_{22}, S_{32}, and S_{12}.

Fig. 16 shows a photograph of the fabricated 2 × 4 filtering Butler matrix. Measurements can be done taking the output port 3 as an example. For this case, the simulated and measured S-parameters of the fabricated 2 × 4 filtering Butler matrix are shown in Fig. 17. It is can be clearly observed that the measured results are in good agreement with the simulation results. The measured minimum insertion loss for the bandpass filter is 8.8 dB, which includes the 6-dB power splitting ratio and 2.8-dB filter loss. The measured return losses are lower than 15 dB, and the isolation between ports 1 and 2 is larger

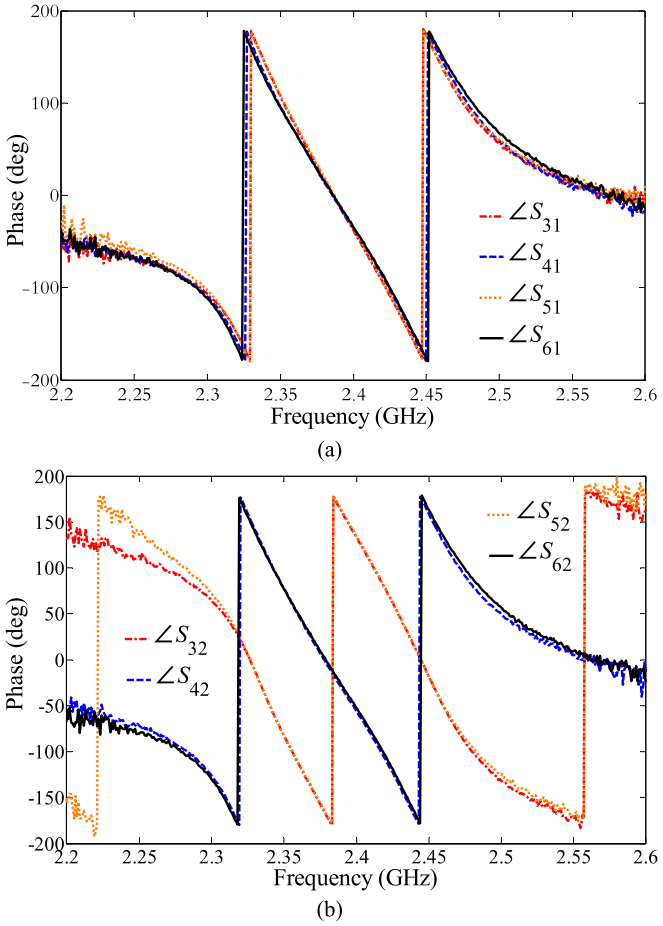

Fig. 18. Measured output phase of the fabricated 2×4 filtering Butler matrix. (a) S_{31}, S_{41}, S_{51}, andS_{61}. (b) S_{32}, S_{42}, S_{52}, and S_{62}.

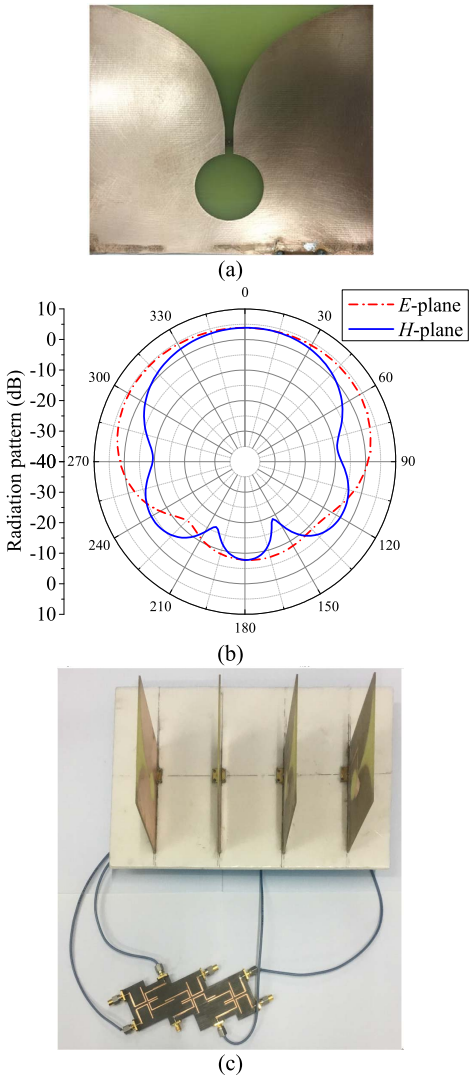

Fig. 19. (a) Antenna element. (b) Simulated radiation patterns of the antenna element used in the linear array. (c) Prototype of the Butler matrix connected to the Vivaldi antenna array.

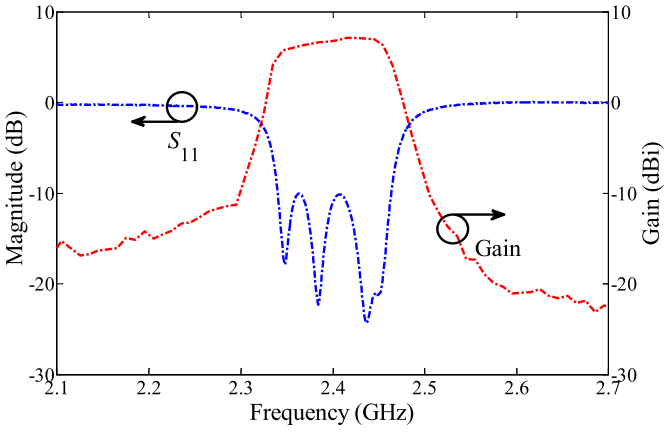

Fig. 20. Measured reflection coefficient and gain of the Vivaldi antenna array when inputting at port 1.

than 25 dB. Similar results are obtained when measurements are done with other port configurations. The measured output phases of the fabricated 2×4 filtering Butler matrix are shown in Fig. 18. When the signal is input from port 1, the phases $\angle S_{31}$, $\angle S_{41}$, $\angle S_{51}$, and $\angle S_{61}$ are almost equal in phase. When the signal is input from port 2, the phases $\angle S_{42}$ and $\angle S_{62}$ are also almost equal in phase, while the phases $\angle S_{32}$ and $\angle S_{52}$ are almost equal out of phase. Within the 3-dBFBW (2.33–2.46 GHz) of the bandpass filter, the measured phase imbalances are within $\pm 9°$.

A switched-beam antenna array has been designed and fabricated to further test the 2×4 filtering Butler matrix. Considering that the radiation element should have a broadband characteristic to cover the bandwidth of the bandpass filter, a Vivaldi antenna is selected to be the radiation element [26]. Fig. 19(a) and (b) shows the simulated antenna radiation patterns in the E- and H-planes. For the test, the four antenna elements have been equally spaced with 62.5-mm gap, which corresponds to 0.5 λ_0 at 2.4 GHz, as shown in Fig. 19(c). Butler matrix is connected to the antenna array by coaxial cables of equal length. Fig. 20 shows the measured reflection coefficient and gain of the Vivaldi antenna array fed by the Butler matrix with port 1 used as the input port. It can be seen that a good filtering characteristic is achieved. Similar performance can be obtained when port 2 is used as the input port. The simulated and measured radiation patterns obtained at 2.4 GHz of the Vivaldi antenna array are shown in Fig. 21. As can be seen, the directions of main beams'

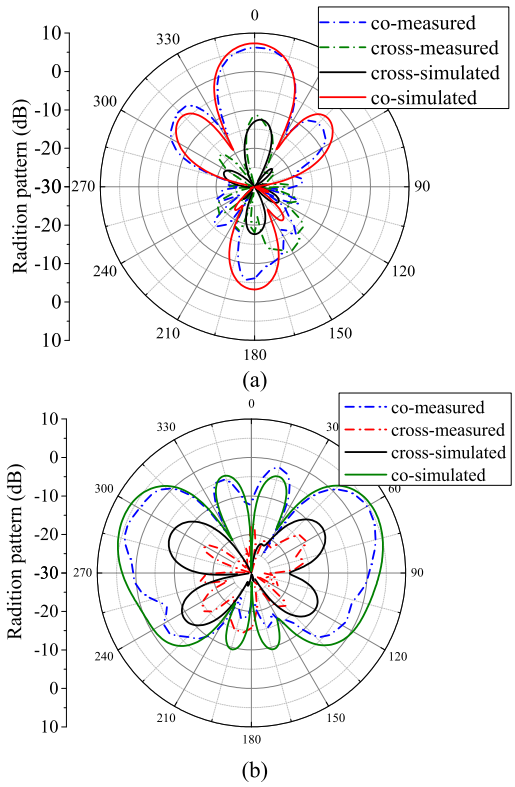

Fig. 21. Simulated and measured radiation patterns at 2.4 GHz while input port at (a) port 1 and (b) port 2.

point at 0° when port 1 is used as the input port, while end-fire performance can be obtained when port 2 is used as the input port. Good agreement has been obtained between the simulation and measured results.

IV. Conclusion

A systematic design procedure of the novel filtering 180° hybrid coupler and its application to the design of a 2 × 4 filtering Butler matrix were presented in this paper. The hybrid coupler is composed of four resonators, which can provide power division, phase shift, and bandpass response. By utilizing the coupling between resonators as the connecting network, a 2 × 4 filtering Butler matrix can be designed easily. For validation, a 180° filtering hybrid coupler and a 2 × 4 filtering Butler matrix are designed, fabricated, and measured. In addition, a Vivaldi antenna array was designed and fabricated to examine the effectiveness of Butler matrix. Close correlation between the simulation and measured results confirms the correctness of the design method. The 2 × 4 Butler matrix can be extended to larger sizes including the classic 4 × 4 array. However, this is subject to further study, as additional phase shifting is required.

References

[1] M.-J. Ho, G. L. Stuber, and M. D. Austin, "Performance of switched-beam smart antennas for cellular radio systems," *IEEE Trans. Veh. Technol.*, vol. 47, no. 1, pp. 10–19, Feb. 1998.

[2] T.-H. Lin, S.-K. Hsu, and T.-L. Wu, "Bandwidth enhancement of 4×4 Butler matrix using broadband forward-wave directional coupler and phase difference compensation," *IEEE Trans. Microw. Theory Techn.*, vol. 61, no. 12, pp. 4099–4109, Dec. 2013.

[3] K. Wincza and S. Gruszczynski, "Broadband integrated 8×8 Butler matrix utilizing quadrature couplers and Schiffman phase shifters for multibeam antennas with broadside beam," *IEEE Trans. Microw. Theory Techn.*, vol. 64, no. 8, pp. 2596–2604, Aug. 2016.

[4] K. Wincza, K. Staszek, I. Slomian, and S. Gruszczynski, "Scalable multibeam antenna arrays fed by dual-band modified Butler matrices," *IEEE Trans. Antennas Propag.*, vol. 64, no. 4, pp. 1287–1297, Apr. 2016.

[5] K. Wincza, S. Gruszczynski, and K. Sachse, "Broadband planar fully integrated 8×8 Butler matrix using coupled-line directional couplers," *IEEE Trans. Microw. Theory Techn.*, vol. 59, no. 10, pp. 2441–2446, Oct. 2011.

[6] J. Allen, "A theoretical limitation on the formation of lossless multiple beams in linear arrays," *IRE Trans. Antennas Propag.*, vol. AP-9, no. 4, pp. 350–352, Jul. 1961.

[7] J. Shelton and K. S. Kelleher, "Multiple beams from linear arrays," *IRE Trans. Antennas Propag.*, vol. AP-9, no. 2, pp. 154–161, Mar. 1961.

[8] H. Moody, "The systematic design of the Butler matrix," *IEEE Trans. Antennas Propag.*, vol. AP-12, no. 6, pp. 786–788, Nov. 1964.

[9] M. Ueno, "A systematic design formulation for Butler matrix applied FFT algorithm," *IEEE Trans. Antennas Propag.*, vol. AP-29, no. 3, pp. 496–501, May 1981.

[10] D. M. Pozar, *Microwave Engineering*, 3rd ed. New York, NY, USA: Wiley, 2005.

[11] T. Macnamara, "Simplified design procedures for Butler matrices incorporating 90° hybrids or 180° hybrids," *Proc. Inst. Elect. Eng.—Microw., Antennas Propag.*, vol. 134, no. 1, pt. H, pp. 50–54, Feb. 1987.

[12] H. Uchida, N. Yoneda, Y. Konishi, and S. Makino, "Bandpass directional couplers with electromagnetically-coupled resonators," in *IEEE MTT-S Int. Microw. Symp. Dig.*, Jun. 2006, pp. 1563–1566.

[13] W.-L. Chang, T.-Y. Huang, T.-M. Shen, B.-C. Chen, and R.-B. Wu, "Design of compact branch-line coupler with coupled resonators," in *Proc. Asia–Pacific Microw. Conf.*, Dec. 2007, pp. 1–4.

[14] C.-K. Lin and S.-J. Chung, "A compact filtering 180° hybrid," *IEEE Trans. Microw. Theory Techn.*, vol. 59, no. 12, pp. 3030–3036, Dec. 2011.

[15] C.-F. Chen, T.-Y. Huang, C.-C. Chen, W.-R. Liu, T.-M. Shen, and R.-B. Wu, "A compact filtering rat-race coupler using dual-mode stub-loaded resonators," in *IEEE MTT-S Int. Microw. Symp. Dig.*, Jun. 2012, pp. 1–3.

[16] W.-R. Liu, T.-Y. Huang, C.-F. Chen, T.-M. Shen, and R.-B. Wu, "Design of a 180-degree hybrid with Chebyshev filtering response using coupled resonators," in *IEEE MTT-S Int. Microw. Symp. Dig.*, Jun. 2013, pp. 1–3.

[17] L.-S. Wu, B. Xia, W.-Y. Yin, and J. Mao, "Collaborative design of a new dual-bandpass 180° hybrid coupler," *IEEE Trans. Microw. Theory Techn.*, vol. 61, no. 3, pp. 1053–1066, Mar. 2013.

[18] U. Rosenberg, M. Salehi, S. Amari, and J. Bornemann, "Compact multi-port power combination/distribution with inherent bandpass filter characteristics," *IEEE Trans. Microw. Theory Techn.*, vol. 62, no. 11, pp. 2659–2672, Nov. 2014.

[19] T. F. Skaik, M. J. Lancaster, and F. Huang, "Synthesis of multiple output coupled resonator circuits using coupling matrix optimisation," *IET Microw., Antennas Propag.*, vol. 5, no. 9, pp. 1081–1088, Jun. 2011.

[20] F. Lin, Q.-X. Chu, and S. W. Wong, "Design of dual-band filtering quadrature coupler using $\lambda/2$ and $\lambda/4$ resonators," *IEEE Microw. Wireless Compon. Lett*, vol. 22, no. 11, pp. 565–567, Nov. 2012.

[21] K. Song, X. Ren, F. Chen, and Y. Fan, "Compact in-phase power divider integrated filtering response using spiral resonator," *IET Microw., Antennas Propag.*, vol. 8, no. 4, pp. 228–234, Mar. 2014.

[22] K. Song, F. Zhang, F. Chen, and Y. Fan, "Synthesis and design method of bandpass-response power divider," *Microelectron. J.*, vol. 45, no. 1, pp. 71–77, 2014.

[23] V. Tornielli di Crestvolant, P. M. Iglesias, and M. J. Lancaster, "Advanced Butler matrices with integrated bandpass filter functions," *IEEE Trans. Microw. Theory Techn.*, vol. 63, no. 10, pp. 3433–3444, Oct. 2015.

[24] J. B. Thomas, "Cross-coupling in coaxial cavity filters—A tutorial overview," *IEEE Trans. Microw. Theory Techn.*, vol. 51, no. 4, pp. 1368–1376, Apr. 2003.

[25] J. S. Hong and M. J. Lancaster, *Microstrip Filters for RF/Microwave Applications*. New York, NY, USA: Wiley, 2001.

[26] C. A. Balanis, *Antenna Theory: Analysis and Design*, 2nd ed. New York, NY, USA: Wiley, 1997.

Qiang Shao was born in Xianning, Hubei, China, in 1993. He received the B.S. degree in information engineering from Shantou University, Shantou, China, in 2015. He is currently pursuing the Ph.D. degree at the South China University of Technology, Guangzhou, China.

His current research interests include microwave filters and associated RF circuits for microwave and millimeter-wave applications.

Fu-Chang Chen (M'12) was born in Fuzhou, Jiangxi, China, in 1982. He received the Ph.D. degree from the South China University of Technology, Guangzhou, China, in 2010.

He is currently a Professor with the School of Electronic and Information Engineering, South China University of Technology. His current research interests include the synthesis theory and the design of microwave filters and associated RF modules for microwave and millimeter-wave applications.

Qing-Xin Chu (M'99–SM'11) received the B.S., M.E., and Ph.D. degrees in electronic engineering from Xidian University, Xi'an, China, in 1982, 1987, and 1994, respectively.

From 1982 to 2004, he was with the School of Electronic Engineering, Xidian University, where he has been a Professor and the Vice Dean since 1997, and a Distinguished Professor of the Shaanxi Hundred-Talent Program since 2011. He is currently a Chair Professor with the School of Electronic and Information Engineering, South China University of Technology, Guangzhou, China, where he is also the Director of the Research Institute of Antennas and RF Techniques and the Chair of the Engineering Center of Antennas and RF Techniques of Guangdong Province. He has authored over 30 invention patents of China and over 300 papers in journals and conferences, which were indexed in SCI more than 1500 times. His current research interests include antennas in wireless communication, microwave filters, spatial power combining array, and numerical techniques in electromagnetics.

Dr. Chu was the recipient of the Science Award by Guangdong in 2013, the Science Awards by the Education Ministry of China in 2008 and 2002, respectively, the Fellowship Award by the Japan Society for Promotion of Science in 2004, and the Educational Award by Shaanxi in 2003. He was a recipient of the Singapore Tan Chin Tuan Exchange Fellowship Award in 2003. He is the Foundation Chair of the IEEE Guangzhou AP/MTT Chapter and a Senior Member of the China Electronic Institute. One of his papers published in the IEEE TRANSACTIONS ON ANTENNAS AND PROPAGATIONS in 2008 becomes the top Essential Science Indicators paper within 10 years in the field of antennas (SCI indexed self-excluded in the antenna field ranged top 1%). In 2014, he was elected as highly cited scholar by Elsevier in the field of electrical and electronic engineering.

Michael J. Lancaster (M'91–SM'04) was born in Keighley, U.K., in 1958. He received the B.Sc. degree in physics and Ph.D. degree in nonlinear underwater acoustics from Bath University, Bath, U.K., in 1980 and 1984, respectively.

He joined the Surface Acoustic Wave (SAW) Group, Department of Engineering Science, Oxford University, Oxford, U.K., as a Research Fellow, where his research concerned the design of new novel SAW devices including filters and filter banks. In 1987, he joined the Department of Electronic and Electrical Engineering, University of Birmingham, Birmingham, U.K., as a Lecturer, where he lectures on electromagnetic theory and microwave engineering, and then began the study of the science and applications of high-temperature superconductors, focusing mainly on microwave frequencies. In 2000, he became the Head of the Emerging Device Technology Research Centre, and in 2003, he became the Head of the Department of Electronic, Electrical and Computer Engineering, University of Birmingham. He has authored or co-authored over 170 papers in refereed journals and 2 books. His current research interests include microwave filters and antennas and the high-frequency properties and applications of a number of novel and diverse materials.

Dr. Lancaster is Fellow of the IET and the U.K. Institute of Physics. He is a Chartered Engineer and Chartered Physicist. He has served on the IEEE Microwave Theory and Techniques International Microwave Symposium Technical Committee.